Available online at www.sciencedirect.com
ScienceDirect
Journal of Non-Crystalline Solids 354 (2008) 2416–2420
JOURNAL OF NON-CRYSTALLINE SOLIDS
www.elsevier.com/locate/jnoncrysol

Comparison of photoluminescence and capacitance spectroscopies as efficient tools for interface characterisation of heterojunction solar cells

R. Chouffot [a], S. Ibrahim [a], R. Brüggemann [b,*], A.S. Gudovskikh [a,c], J.P. Kleider [a], M. Scherff [d], W.R. Fahrner [d], P. Roca i Cabarrocas [e], D. Eon [e], P.-J. Ribeyron [f]

[a] *Laboratoire de Génie Electrique de Paris, CNRS UMR8507; SUPELEC; Univ Paris-Sud; UPMC Univ Paris 06; 11 rue Joliot-Curie, Plateau de Moulon, F-91192 Gif-sur-Yvette Cedex, France*
[b] *Institut für Physik, Carl von Ossietzky Universität Oldenburg, D-26111 Oldenburg, Germany*
[c] *Saint-Petersburg Physics and Technology Centre for Research and Education of the Russian Academy of Sciences, Hlopina str. 8/3, Saint Petersburg 195220, Russia*
[d] *Lehrgebiet Bauelemente der Elektrotechnik, Fern-Universität Hagen, D-58084 Hagen, Germany*
[e] *Laboratoire de Physique des Interfaces et des Couches Minces, UMR 7647, CNRS, Ecole Polytechnique, F-91128 Palaiseau cedex, France*
[f] *INES-CEA, 17 rue des Martyrs, F-38054 Grenoble cedex 9, France*

Available online 20 February 2008

Abstract

The correlation between diffusion capacitance and photoluminescence as a method of interface-defect density characterisation in amorphous silicon/crystalline silicon heterojunction solar cells is explored by numerical modelling and experimentally. At open circuit, the influence of the defect density at the front amorphous silicon/crystalline silicon interface and the surface recombination velocity of the minority carriers in the bulk depend on the doping level of the crystalline silicon and the critical contribution of the majority carriers. Experimental illustration is given for five series of solar cells with different doping levels, interface properties and back contacts. We observe agreement between simulation and experimental results and a correlation between the two methods of measurement of interface defects.

PACS: 72.40.+w; 73.20.−r; 73.40.Lq; 78.55.−m; 84.37.+q

Keywords: Silicon; Solar cells; Heterojunctions; Photovoltaics; Optical spectroscopy; Defects; Modeling and simulation

1. Introduction

Heterojunctions between hydrogenated amorphous silicon (a-Si:H) and crystalline silicon (c-Si) are of great interest for the photovoltaic development owing to the possibility of conversion efficiencies in excess of 20% [1]. However, a good quality of the front interface of such devices is essential [2] and there is a strong need for capable characterisation techniques.

Photoluminescence is a tool [3,4] which allows probing of the properties of the front interface and back contact. By measurement of the radiative recombination of the excess carriers in the volume, information is extracted on recombination losses at the heterojunction interface and/or the back contact. A recent method of interface defect characterisation is based on the measurement of the low-frequency diffusion capacitance at forward bias close to the open-circuit voltage, under AM1.5 illumination [5,6]. In this paper, we apply both photoluminescence and capacitance techniques

* Corresponding author.
E-mail address: rudi.brueggemann@uni-oldenburg.de (R. Brüggemann).

0022-3093/$ - see front matter © 2007 Elsevier B.V. All rights reserved.
doi:10.1016/j.jnoncrysol.2007.09.032

on heterojunction solar cells and correlate the experimental with simulation results from numerical modelling of the experiments.

2. Experiment and simulation details

The electrical measurements were performed on different series of a-Si:H/c-Si heterojunction solar cells for which Table 1 gives information on the structures and doping levels. The interface properties of the front a-Si:H(n)/c-Si(p) interface are different between the samples of the same series on account of different surface treatment processes and a-Si:H deposition conditions.

Capacitance measurements were performed using an HP4284A impedance meter in the frequency range of 20 Hz–1 MHz. The samples were illuminated by an equivalent AM1.5D spectral flux. The temperature of the cells was regulated by a Peltier module and set at 300 K. The cells were forward-biased using a Keithley 2400 source meter. The applied bias is close to the open-circuit voltage (V_{oc}) of the cell in order to reduce the current passing through the cell and to allow reliable capacitance measurements. Indeed, we know from previous work that the capacitance exhibits a low-frequency plateau, C_{LF}, which reflects the quality of the interface [7].

The photoluminescence (PL) measurements were performed at room temperature at open-circuit conditions using excitation from an 850-nm laser diode. The luminescence was collected and dispersed by a monochromator and measured by a LN-cooled InGaAs detector using a lock-in technique.

A new simulation tool, developed at Laboratoire de Génie Electrique de Paris, was used to reproduce and analyse the PL and C_{LF} measurements for a-Si:H(n)/c-Si(p) heterojunction solar cells with different interface qualities under AM1.5D illumination. Interface defects were modelled by introducing a layer of 1 nm thickness of crystalline silicon at the interface containing a high density of defect states. Defects were introduced as a Gaussian distribution centred at 0.7 eV above the valence-band edge, with a standard deviation of 0.1 eV. The integrated interface state density (N_{if}) was varied between $2.5 \times 10^{10}\,cm^{-2}$ and $2.5 \times 10^{12}\,cm^{-2}$. Both types of defects (acceptor or donor) were probed in the simulation. However, the general trends were the same and results will be shown only for acceptor states in the following. The effect of other important cell parameters was also taken into consideration. In particular, the simulations were performed for two values of bulk doping representing the average resistivity of our c-Si wafers ($N_a = 7 \times 10^{14}\,cm^{-3}$, $N_a = 10^{16}\,cm^{-3}$), and for two extreme values of minority-carrier (electron) back-surface recombination velocities ($S_{bn} = 10^7\,cm\,s^{-1}$, $S_{bn} = 10^2\,cm\,s^{-1}$). The back-surface recombination velocity for majority carriers (holes) was set at $S_{bp} = 10^7\,cm\,s^{-1}$ in all simulations. The integrated photoluminescence (iPL) was determined from the integration of PL spectra that were calculated with Kirchhoff's generalised law [8], which takes into account the spatial variation of the quasi-Fermi levels for electrons and holes, E_{fn} and E_{fp}, and the optical reflectivities of the front and rear interfaces of the solar cell.

Table 1
Summary of parameters for the heterojunction solar cells

Series	Wafer resistivity (Ω cm)	Rear contact	Remarks
SAH	1	Al	
SAM	3	Al	Textured
SBH	1	Diffused BSF	
SBL	14–22	Al BSF	
DHJ	14–22	a-Si:H(p)/Al BSF	

BSF means a so-called back-surface field (BSF) layer.

3. Results

For the two doping levels and the two S_{bn} values, the iPL measured at open circuit is shown versus V_{oc} in Fig. 1. The different data points were obtained by changing N_{if} from $2.5 \times 10^{10}\,cm^{-2}$ to $2.5 \times 10^{12}\,cm^{-2}$, where the increase of defect density implies a decrease of V_{oc} and PL yield. In Fig. 2, we present the calculated C_{LF} at V_{oc} under AM1.5D illumination versus V_{oc}.

Figs. 1 and 2 show that both iPL and C_{LF} increase with V_{oc}, as a result of a decrease of interface defect density. The behaviour is roughly the same between the two methods of interface defects characterisation. In order to compare the two methods, the variation of the calculated C_{LF} versus iPL is shown in Fig. 3.

The summary of experimental data in terms of PL detector signal at 1130 nm versus C_{LF} for the different series of samples is shown in Fig. 4, where each series is represented by a different symbol.

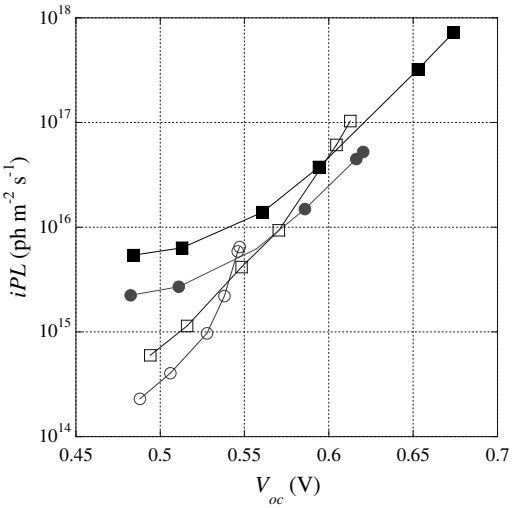

Fig. 1. Calculated iPL versus V_{oc} for a simple a-Si:H(n)/c-Si(p) heterojunction for variation of N_{if}. The circle data points correspond to $S_{bn} = 10^7$ cm/s and the square data points correspond to $S_{bn} = 10^2$ cm/s. The filled (open) symbols correspond to a doping level of $10^{16}\,cm^{-3}$ ($7 \times 10^{14}\,cm^{-3}$). The lines are guides to the eye.

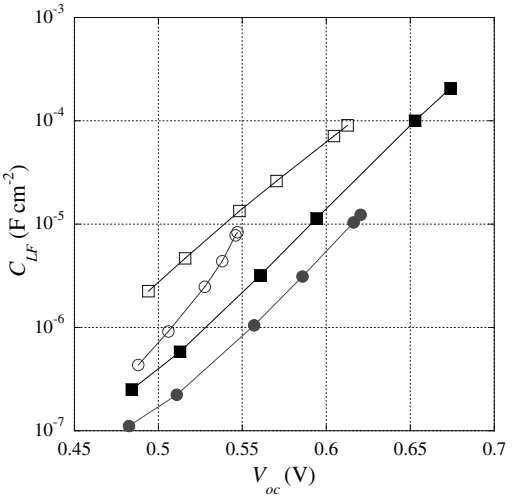

Fig. 2. Calculated C_{LF} versus V_{oc} for the same parameters and symbols as in Fig. 1.

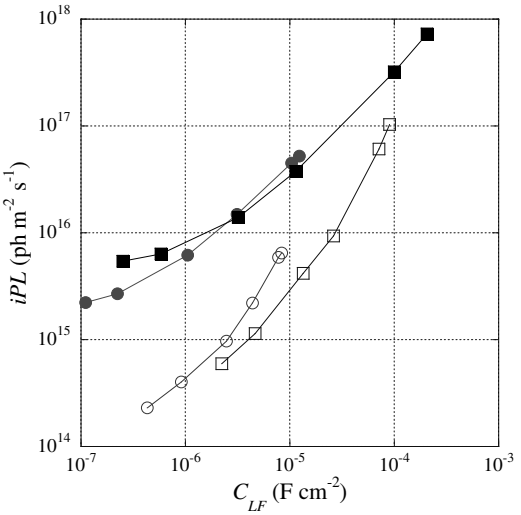

Fig. 3. Calculated iPL versus calculated C_{LF}. The symbols and parameters correspond to those in Fig. 1.

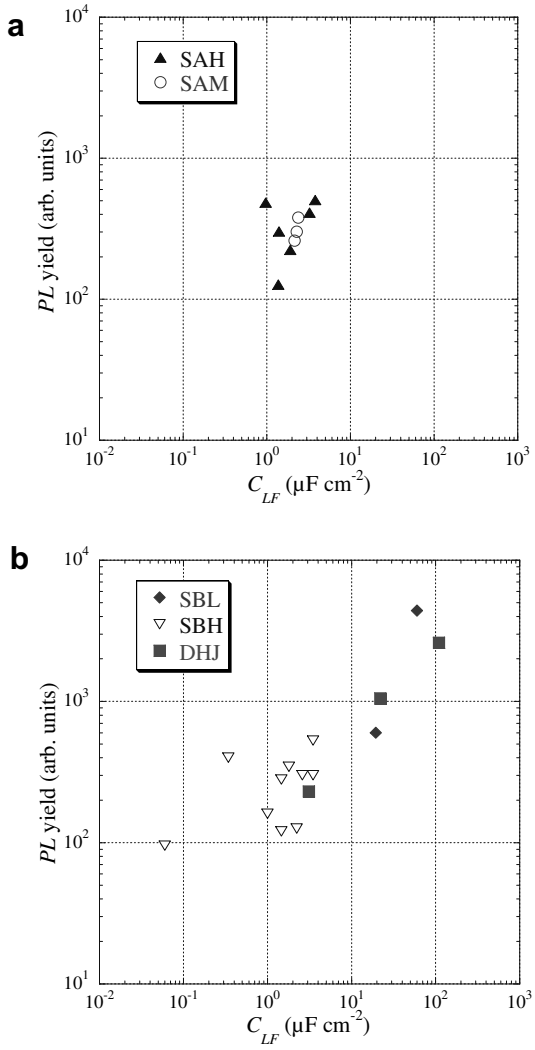

Fig. 4. Measured PL yield versus measured C_{LF} for the five series of sample cells. For SAH and SAM series, the *PL* yield measurements are made under excitation wavelength of 780 nm (a), and for SBL, SBH and DHJ series, the excitation wavelength is 850 nm (b). The excitation photon flux was a factor of six higher in (a) than in (b).

4. Discussion

We first discuss the effect of front-interface defect density on the simulated iPL for the high-doping case. The tendency in Fig. 1 for high or low S_{bn} is similar but the increase in S_{bn} results in lower iPL and quasi-Fermi level splitting and thus lower V_{oc} because of enhanced minority-carrier loss at the rear contact.

For lower values of N_{if}, that means higher V_{oc}, Fig. 1 identifies an exponential dependence of iPL on V_{oc}: iPL $\propto \exp[eV_{oc}/(kT)]$, e being equal to 1.6×10^{-19} C, k being Boltzmann's constant and T being the temperature. The value of iPL directly depends on the integral of the product of carrier concentrations, np, in the bulk.

In Fig. 5, we present the profile of the quasi-Fermi level splitting, E_{Fn}–E_{Fp}, in the cell, for different values of N_{if} and for $S_{bn} = 100$ cm/s. For low values of N_{if}, the concentration of the minority carriers, n, is constant in the c-Si layer ($x > 10^{-6}$ cm), while the concentration of the holes, p, remains constant and equal to the equilibrium value corresponding to the doping density. The quasi-Fermi level splitting is independent of the position in c-Si and is equal to eV_{oc}, which then leads to the observed exponential dependence for iPL.

For the highest N_{if} values corresponding to the low values of V_{oc} (between 470 mV and 520 mV), iPL in Fig. 1 deviates from the exponential dependence on V_{oc} and tends to saturate. In this high front-interface defect density range, the quasi-Fermi level splitting close to the interface ($x < 5 \times 10^{-2}$ cm) still decreases when the interface-defect density increases, leading to lower V_{oc} values. However, the quasi-Fermi level splitting in the bulk region ($x > 5 \times 10^{-2}$ cm) is almost unchanged due to the generation of carriers in the bulk. This explains that iPL almost

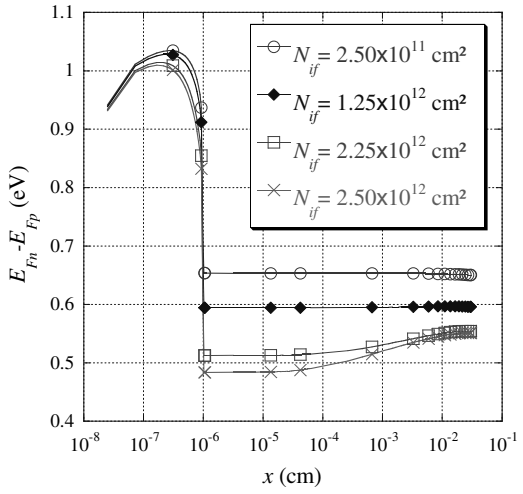

Fig. 5. Calculated quasi-Fermi level splitting E_{Fn}–E_{Fp} versus thickness (x) of the cell for a doping level of 10^{16} cm^{-3} and $S_{bn} = 10^2$ cm/s. The interface position is at $x = 10^{-6}$ cm. The quasi-Fermi level splittings are plotted for different values of N_{if} in the range of 2.5×10^{11} cm^{-2} to 2.5×10^{12} cm^{-2}.

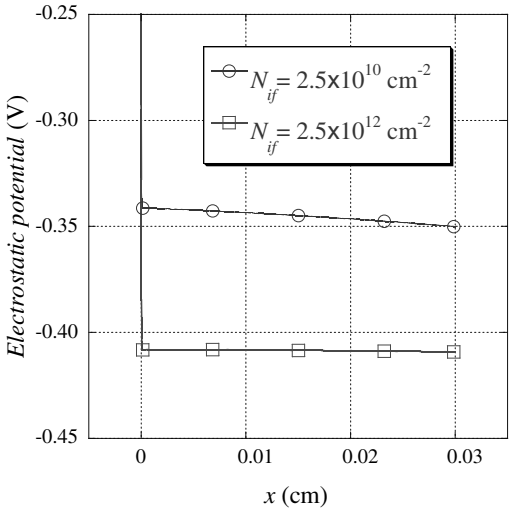

Fig. 6. Simulated electrostatic potential versus thickness (x) for doping level of 7×10^{14} cm^{-3}, $S_{bn} = 10^7$ cm/s and N_{if} of 2.5×10^{10} cm^{-2} and 2.5×10^{12} cm^{-2}. The heterojunction is on the left.

saturates, since the main contribution to iPL comes from recombination in the bulk. These results are similar to the case reported by Bauer et al. [4] for ohmic back contacts.

We now discuss the simulated low-doping iPL results. In Fig. 1, the slope of ln(iPL) versus V_{oc} increases for higher V_{oc}, i.e., for low N_{if}, compared to the high-doping case. While the values of E_{Fn}–E_{Fp} close to the front interface still determine the variation of iPL, they become higher than eV_{oc} and vary more strongly with increasing V_{oc} than $\exp[eV_{oc}/(kT)]$. For this low-doping case, the concentration of majority carriers under illumination becomes higher than the doping concentration because of the excess carriers. At V_{oc}, the net current density is zero but internally partial hole and electron currents are driven by the gradients of E_{Fp} and E_{Fn}. At high N_{if}, the electron density is low enough that a very small gradient in E_{Fp} is sufficient and the electrostatic potential drop across the c-Si, illustrated in Fig. 6, is negligible and iPL follows $\exp[eV_{oc}/(kT)]$. At low N_{if}, the electron density is higher, leading to a more significant drop in the electrostatic potential (Fig. 6), which is equal to $(E_{Fn}–E_{Fp})/e - V_{oc}$. In fact, this electrostatic-potential drop imposes a limitation to V_{oc} and reduces its value.

We now discuss the effect of N_{if} on the simulated C_{LF}. In Fig. 2, the behaviour is analogous to that of iPL, with an exponential dependence of C_{LF} on V_{oc}: $C_{LF} \propto \exp[e\ V_{oc}/(kT)]$. However, as opposed to iPL, this exponential dependence holds in the whole range of V_{oc} without any clear saturation at low V_{oc}. This is because bulk generation has less influence on the capacitance than on the photoluminescence. Indeed, the capacitance results from a change of the out-of-phase component of the current subsequent to the change of bias voltage (which is sinusoidally modulated). Thus it is not directly related to the integrated carrier densities like iPL but to their bias-induced changes. For the low-doping case, we can observe the same behaviour as in iPL due to the electrostatic potential drop at the back contact.

Going further into the correlation between the photoluminescence and capacitance methods with the help of Fig. 3, we observe that for the high-doping case, there is a well-defined linear dependence between iPL and C_{LF} at low defect densities. There is a deviation from this linear dependence at high defect densities due to the saturation of iPL.

The simulation results of Fig. 3 can directly be related to the experimental results in Fig. 4. We observe a linear trend between C_{LF} and PL values for the results of the different series of samples. In the range between 4 and 10 μF cm^{-2} for C_{LF} in Fig. 3, the results for the two S_{bn} are similar with a lower N_{if} corresponding to $S_{bn} = 10^7$ cm/s. To put this observation in another way, the samples without back-surface field (BSF) require a lower N_{if} for the same values of C_{LF} and PL. This argument suggests that N_{if} may be lower for most of the samples of SAH series and SAM series samples than for the BSF samples. On the other hand, only the BSF samples achieve the high values of C_{LF} which indicates low N_{if}. One SBH sample falls into the range in which the PL yield saturates so that a high N_{if} can be attributed to this solar cell (with a V_{oc} of only 512 mV).

5. Conclusions

Comparison between diffusion capacitance and photoluminescence measurements as methods of characterisation of a-Si:H/c-Si interface solar cells has shown a good correlation between simulation and experimental results. The simulation results identified the influence of both interface-defect density and back contact on the value of V_{oc}

and on the capacitance and photoluminescence. For doping levels in the range of $7 \times 10^{14}\,cm^{-3}$, the limitation imposed on the open-circuit voltage by an electrostatic-potential drop under the influence of the excess majority carriers was related to the simulated photoluminescence and capacitance measurements.

Acknowledgements

This work was partly supported by ANR (Agence Nationale de la Recherche) in the framework of the French national photovoltaic PHARE project, as well as by a French-German Procope program, funded by DAAD, Bonn, and Egide, Paris. Rémy Chouffot would like to thank ADEME (Agence De l'Environnement et de la Maîtrise de l'Energie) and CNRS (Centre National de Recherche Scientifique) for financial support during his PhD.

References

[1] M. Tanaka, S. Okamoto, S. Tsuge, S. Kiyama, in: K. Kurokawa et al. (Eds.), Proceedings of the 3rd World Conference on Photovoltaic Energy Conversion, Osaka, Japan, May 2003, p. 955.
[2] K. von Maydell, H. Windgassen, W.A. Nositschka, U. Rau U., P.J. Rostan, J. Henze, J. Schmidt, M. Scherff, W. Fahrner, D. Borchert, S. Tardon, R. Brüggemann, H. Stiebig, M. Schmidt, in: W. Palz et al. (Eds.), Proceedings of Twentieth European Photovoltaic Solar Energy Conference, Barcelona, Spain, 6-10 June 2005, WIP, Munich, 2005, p. 822.
[3] S. Tardon, M. Rösch, R. Brüggemann, T. Unold, G.H. Bauer, J. Non-Cryst. Solids 338&340 (2004) 444.
[4] G.H. Bauer, S. Tardon, M. Rösch, T. Unold, Phys. Status Solidi (c) 1 (2004) 1308.
[5] A.S. Gudovskikh, J.P. Kleider, J. Damon-Lacoste, P. Roca i Cabarrocas, Y. Veschetti, J.-C. Muller, P.-J. Ribeyron, E. Rolland, Thin Solid Films 511&512 (2006) 385.
[6] A.S. Gudovskikh, J.P. Kleider, R. Stangl, J. Non-Cryst. Solids 352 (2006) 1213.
[7] A.S. Gudovskikh, J.P. Kleider, Appl. Phys. Lett. 90 (2007) 034104.
[8] P. Würfel, Physics of Solar Cells, Wiley-VCH, Weinheim, 2005.